

Supporting information

2D luminescent metal-organic framework : efficiently and highly selective detection of 2,4,6-trinitrophenol at ppb level

Ming Yue Fan,^{a‡} Peng Fu,^{a,c‡} Jiao Li,^b Zhong Min Su,^{*a,c} Xiao Li,^{*a,c} Qing Qing Pan,^{a,c} Xiao Li Hu^{a,c}

a. School of Chemical and Environmental Engineering, Changchun University of Science and Technology, Changchun 130022, People's Republic of China.

b. School of Materials science and Engineering, Changchun University of Science and Technology, Changchun 130022, People's Republic of China.

c. Jilin Provincial Science and Technology Innovation Center of Optical Materials and Chemistry, Changchun University of Science and Technology, Changchun, 130022, People's Republic of China.

Corresponding author

* E-mail: zmsu@nenu.edu.cn lix@cust.edu.cn;

1. Materials and measurement

All reagents and solvents for the syntheses were purchased from commercial sources and used as received, unless otherwise indicated. And 9,10-bis(*N*-benzimidazolyl)-anthracene (**L**) were synthesized according to the literature¹. Infrared spectra were obtained from KBr pellets in a wavelength ranging from 4000-400 cm⁻¹ on a Nicolet 380 FT-IR spectrophotometer and UV-Vis absorption was performed on U-3010 spectrophotometer (Hitachi, Japan). Photoluminescence spectra were recorded on a FL-4600 FL spectrophotometer. Powder X-Ray diffraction (PXRD) patterns were

acquired on a Siemens D5005 automated diffractometer with Cu Ka ($\lambda = 1.5418 \text{ \AA}$) radiation. Thermogravimetric analysis (TGA) was conducted on a Perkin-Elmer FLS-920 analyzer heated from ambient temperature to 1000 °C under argon atmosphere at a ramp rate of 5 °C min⁻¹. Emission lifetime measurements were performed on photon technology international quanta master/time master TM 400 phosphorescence/fluorescence Spectrofluorometer.

2.2 X-ray crystallographic analysis

The crystal data of **CUST-531** was collected at room temperature using a Bruker D8 VENTURE diffractometer with ω -scanning technology under graphite monochromatic Mo K α radiation ($\lambda = 0.71073 \text{ \AA}$). The original data was obtained by SHELXL-97 crystallography software using full matrix least square method based on F^2 to obtain accurate crystal structure.² All non-hydrogen atoms were anisotropically refined. The relevant data details are shown in **Table S1** and **Table S2**. CCDC number is **2040004**.

Table S1. Crystal Data and Structure Refinements for **CUST-531**.

Crystal data	CUST-531
Empirical formula	C ₂₅ H ₂₁ O ₅ N ₄ Cd
Formula weight	569.86
Temperature/K	296.15
Crystal system	monoclinic
Space group	P2 ₁ /n
a/Å	12.460(14)
b/Å	10.231(10)
c/Å	18.54(2)
$\alpha/^\circ$	90
$\beta/^\circ$	92.34(2)
$\gamma/^\circ$	90

Volume/ \AA^3	2362(4)
Z	4
Goodness-of-fit on F^2	1.050
Final R indexes [$I >= 2\sigma(I)$]	$R_I = 0.0566,$ $wR_2 = 0.1465$
Final R indexes [all data]	$R_I = 0.0891,$ $wR_2 = 0.1673$
$\rho_{\text{cal}} \text{cg/cm}^3$	1.603
μ/mm^{-1}	0.969
F (000)	1148.0
Radiation	Mo K α ($\lambda = 0.71073$)
Index ranges	-14 $\leq h \leq 13,$ -12 $\leq k \leq 10,$ -20 $\leq l \leq 22$
Reflections collected	13589
Independent reflections	4258 [$R_{\text{int}} = 0.0652$ $R_{\text{sigma}} = 0.0667$]
Data/restraints/parameters	4258/60/319
Goodness-of-fit on F^2	1.050
2 Θ range for data collection/ $^\circ$	3.866 to 50.586
Largest diff. peak/hole / e \AA^{-3}	0.95/-1.18

Table S2. Selected bond distances (\AA) and angles ($^\circ$) for **CUST-531**.

Bond	Distance (\AA)
Cd(1)-O(1)#1	2.335(5)
Cd(1)-O(2)#1	2.373(5)
Cd(1)-O(3)	2.216(5)
Cd(1)-O(4)#2	2.288(6)
Cd(1)-N(2)	2.285(7)
Cd(1)-O(5)	2.385(8)

Bond	Angle ($^\circ$)
O(1)#1-Cd(1)-O(2)#1	55.39(15)
O(1)#1-Cd(1)-O(5)	83.4(2)
O(2)#1-Cd(1)-O(5)	82.1(2)
O(3)-Cd(1)-O(1)#1	90.49(18)
O(3)-Cd(1)-O(2)#1	144.82(18)
O(3)-Cd(1)-O(4)#2	117.7(2)
O(3)-Cd(1)-N(2)	102.9(2)
O(3)-Cd(1)-O(5)	86.0(3)
O(4)#2-Cd(1)-O(1)#1	146.84(18)
O(4)#2-Cd(1)-O(2)#1	93.20(17)

O(4)#2-Cd(1)-O(5)	81.7(3)
O(4)#2-Cd(1)-O(1)#1	146.84(18)
O(4)#2-Cd(1)-O(2)#1	93.20(17)
N(2)-Cd(1)-O(1)#1	101.2(2)
N(2)-Cd(1)-O(2)#1	93.1(2)
N(2)-Cd(1)-O(4)#2	89.7(2)
N(2)-Cd(1)-O(5)	169.9(3)

¹+X, 1+Y, +Z; ²1-X, 1-Y, 1-Z; ³+X, -1+Y, +Z; ⁴-X, 1-Y, 1-Z

3. Characterizations and results

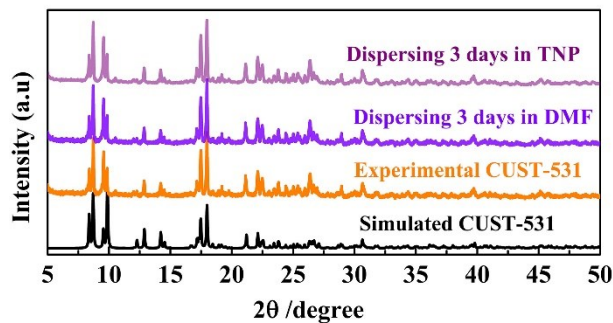


Fig.S1 Powder X-ray diffraction patterns of **CUST-531**.

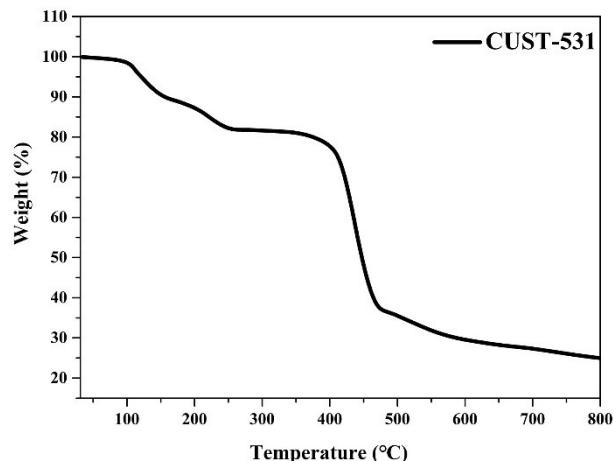


Fig.S2 TG curves of **CUST-531**.

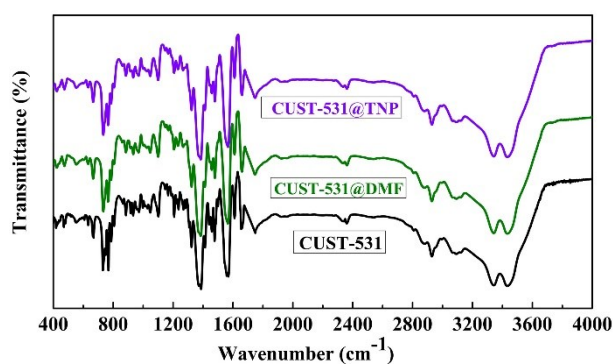


Fig.S3 FTIR spectrum of **CUST-531**.

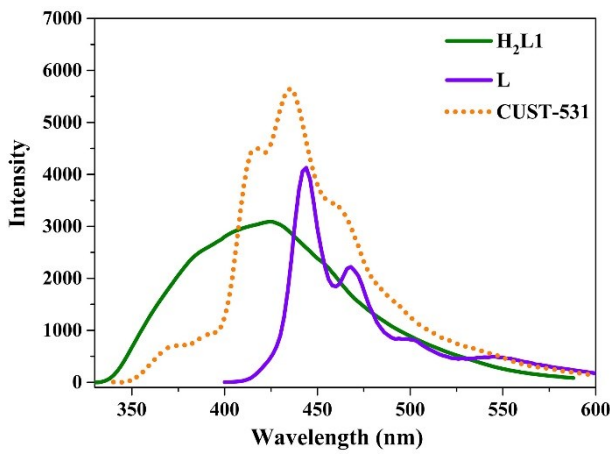


Fig.S4 Solid-state emission spectra of **CUST-531** and free ligands.

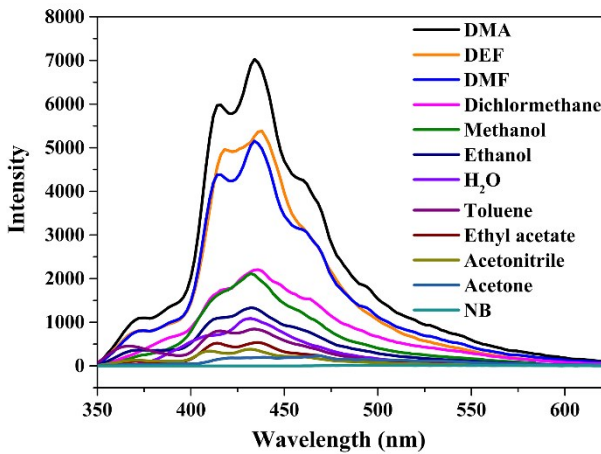


Fig.S5 Photoluminescence spectra of **CUST-531** in different solvents.

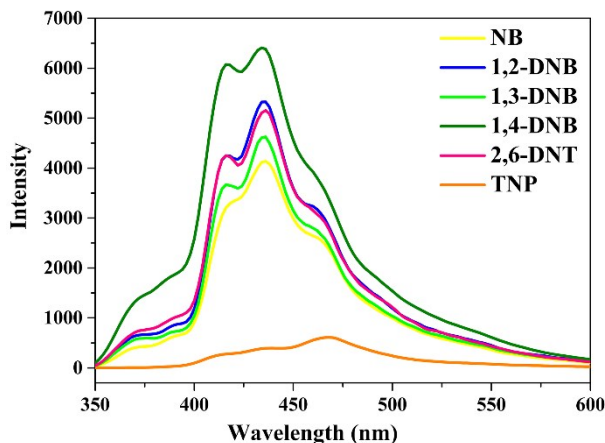


Fig.S6 Photoluminescence spectra of **CUST-531** in DMF containing different nitro analytes (50ppm).

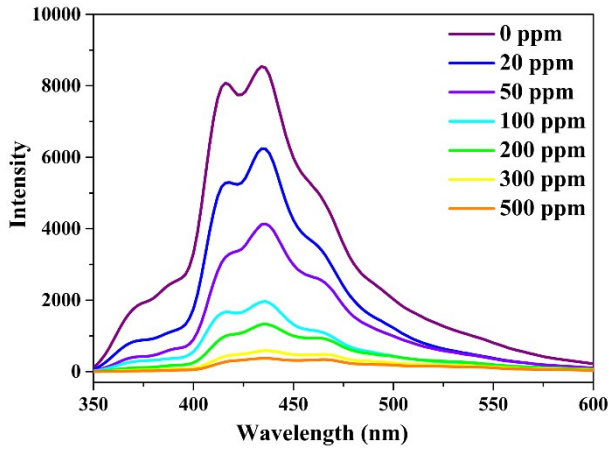


Fig.S7 Photoluminescence spectra of **CUST-531** in DMF containing **NB**.

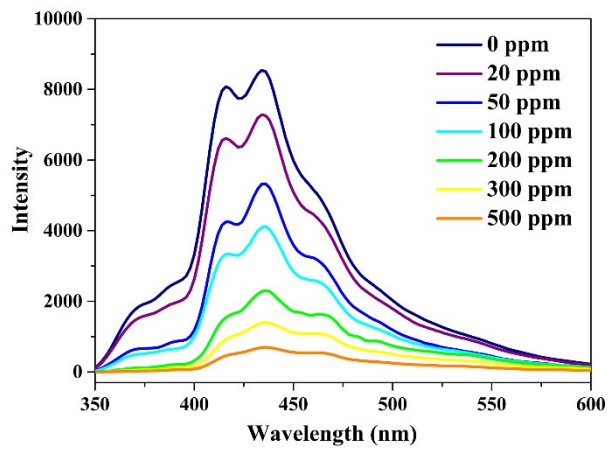


Fig.S8 Photoluminescence spectra of **CUST-531** in DMF containing **1,2-DNB**.

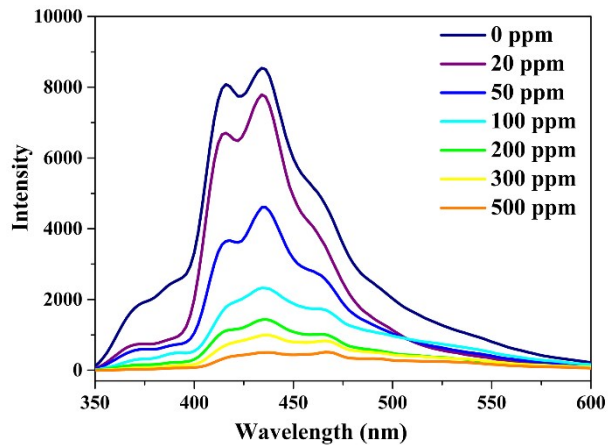


Fig.S9 Photoluminescence spectra of **CUST-531** in DMF containing **1,3-DNB**.

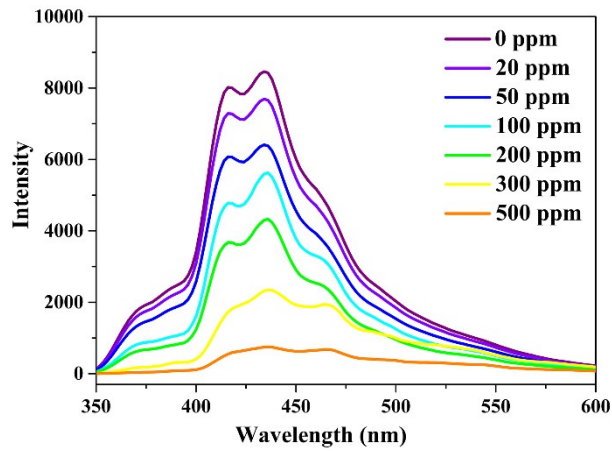


Fig.S10 Photoluminescence spectra of **CUST-531** in DMF containing 1,4-DNB.

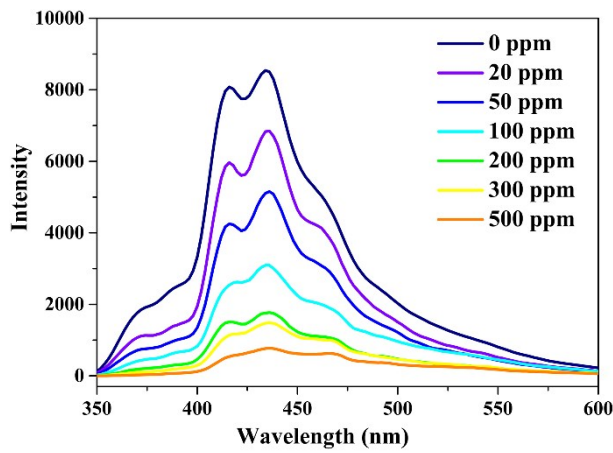


Fig.S11 Photoluminescence spectra of **CUST-531** in DMF containing 2,6-DNT.

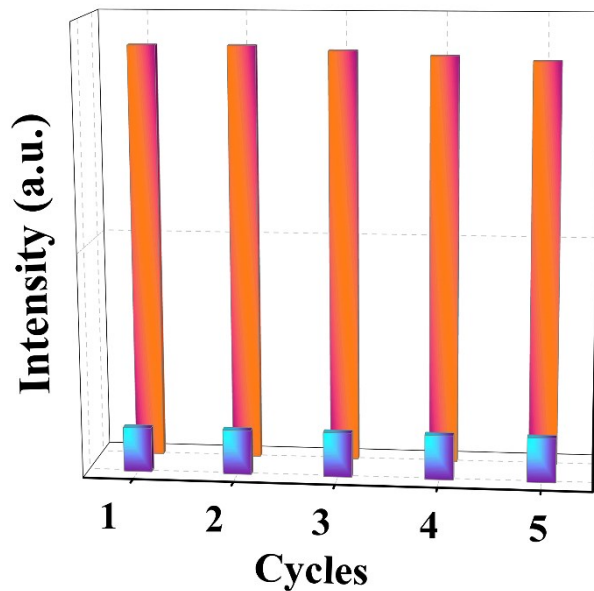


Fig.S12 The quenching and recyclability test of **CUST-531** after sensing TNP.

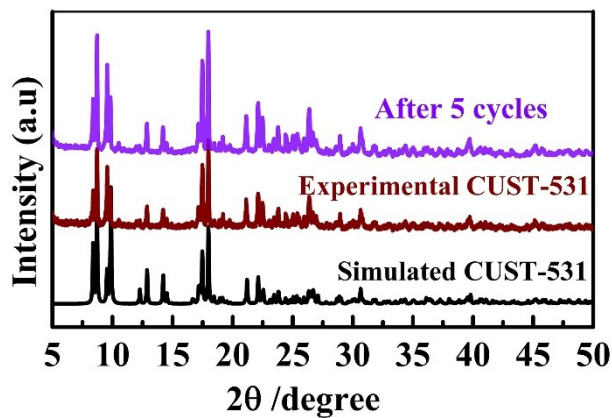


Fig.S13 Powder X-ray diffraction patterns of **CUST-531** in different conditions.

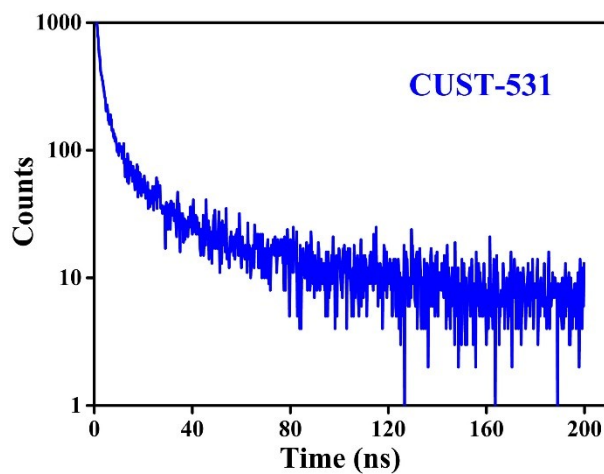


Fig. S14 Lifetime decay curve of **CUST-531** before **TNP** addition.

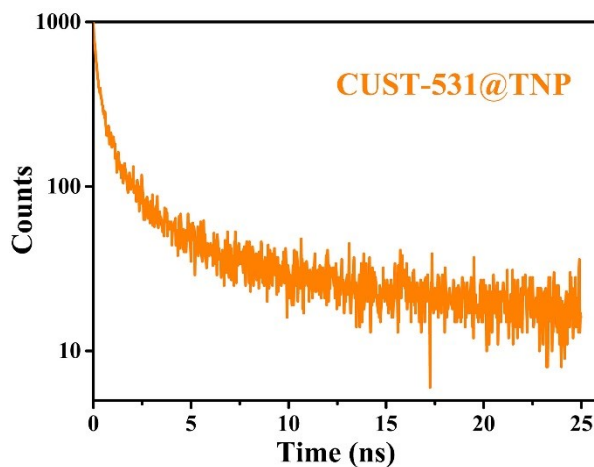


Fig. S15 Lifetime decay curve of **CUST-531** after **TNP** addition.

Table S3. A comparison of the Stern-Volmer constant (K_{SV}), detection limit for the detection of TNP by reported sensors.

MOF	K_{SV}	Detection Limit	Ref.
CUST-531	$3.90 \times 10^5 \text{ M}^{-1}$	29 ppb ($1.28 \times 10^{-7} \text{ M}$)	This work
$[\text{Cd (INA)(pytpy)(OH)} \cdot 2 \text{ H}_2\text{O}]_n$	$4.30 \times 10^4 \text{ M}^{-1}$	$2.41 \mu\text{M}$	[3]
$[\text{Cd}_2(\text{NDC})_{0.5}(\text{PCA})_2]\text{G}_x$	$3.5 \times 10^4 \text{ M}^{-1}$	None	[4]
$\{[\text{Cd}_2(\text{Py2TTz})_2(\text{BDC})_2] \cdot 2(\text{DMF})\}_n$	$3.3 \times 10^4 \text{ M}^{-1}$	$0.93 \mu\text{M}$	[5]
$[\{\text{Cd(fdc)}(\text{bpee})_{1.5}\} \cdot 3(\text{H}_2\text{O})]$	$6.64 \times 10^4 \text{ M}^{-1}$	$5 \mu\text{M}$	[6]
$[\text{Cd}(\text{NDC})\text{L}]_2 \cdot \text{H}_2\text{O}$	$3.7 \times 10^4 \text{ M}^{-1}$	None	[7]
$[\text{Cd(L)}_2] \cdot (\text{DMF})_{0.92}$	$9.3 \times 10^4 \text{ M}^{-1}$	$1.3 \mu\text{M}$	[8]
M1	$0.50 \times 10^4 \text{ M}^{-1}$	$4.70 \mu\text{M}$	[9]

References

1. L. Li, T. L. Hu, J. R. Li, D. Z. Wang, Y. F. Zeng and X. H. Bu. *CrystEngComm*. 2007, **9**, 412-420.
2. G. M. Sheldrick. SHELXL-2014, Program for the Crystal Structure Refinement, University of Göttingen, Germany, 2014.
3. J. Zhang, J. Wu, G. Tang, J. Feng, F. Luo, B. Xu and C. Zhang. *Sensors & Actuators B Chemical*. 2018, **272**, 166-174.
4. S. S. Nagarkar, B. Joarder, A. K. Chaudhari, S. Mukherjee and S. K. Ghosh. *Angew. Chem. Int. Ed.* 2013, **52**, 2881-2885.
5. Z. W. Zhai, S. H. Yang, M. Cao, L. K. Li, C. X. Du and S. Q. Zang. *Cryst. Growth Des.* 2018, **11**, 7173-7182.
6. D. Singh, C. M. Nagaraja. *Cryst. Growth Des.* 2015, **15**, 3356-3365.
7. B. Q. Song, C. Qin, Y. T. Zhang, X. S. Wu, L. Yang, K. Z. Shao and Z. M. Su. *Dalton Trans.* 2015, **44**, 18386-18394.
8. S. Senthilkumar, R. Goswami, V. J. Smith, H. C. Bajaj and S. Neogi. *ACS Sustainable*

Chem. Eng. 2018, **6**, 10295-10306.

9. J. Zhang, L. Gong, J. Feng, J. Wu and C. Zhang. *New J. Chem.* 2017, **41**, 8107-8117.